Chemical Engineering Journal 297 (2016) 158–169

Contents lists available at ScienceDirect

Chemical Engineering Journal

journal homepage: www.elsevier.com/locate/cej

Processing of 2D-MAXene nanostructures and design of high thermal conducting, rheo-controlled MAXene nanofluids as a potential nanocoolant

K.V. Mahesh, Vazhayal Linsha, A. Peer Mohamed, S. Ananthakumar *

Functional Materials Section, Materials Science and Technology Division, Council of Scientific and Industrial Research – National Institute for Interdisciplinary Science and Technology (CSIR-NIIST), Thiruvananthapuram 695019, Kerala, India

HIGHLIGHTS

- 2D Ti_3SiC_2 MAXene nanosheets based nanofluid was developed for the first time.
- This very stable MAXene nanofluid show rheo-controlled flow behavior.
- About 45% enhancement in thermal conductivity was achieved at 323 K.
- The MAXene nanofluid also exhibit lubricating properties.
- These exotic properties make it superior to conventional heat transfer fluids.

GRAPHICAL ABSTRACT

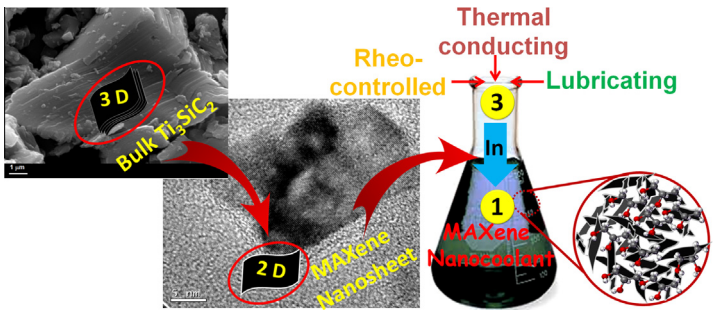

ARTICLE INFO

Article history:
Received 4 February 2016
Received in revised form 22 March 2016
Accepted 2 April 2016
Available online 8 April 2016

Keywords:
2D MAX phase
MAXenes
Ti_3SiC_2
Thermal nanofluids
Thermal conductivity

ABSTRACT

'Nanocoolants' offering extraordinary heat transport property demand new and exotic nanostructures as fillers that can display enhanced thermal conductivity and thermochemical stability for efficient thermal management operations. Herein we report for the first time, the processing of stable MAXene nanofluids using 2D MAXene nanosheets derived from the bulk nanolaminated Ti_3SiC_2 MAX phase ternary carbides via shear induced micromechanical delamination technique. The beneficial multifunctional physical properties of MAXene colloid such as thermal conductivity, viscosity and lubrication effect are assessed and reported. An enhancement of thermal conductivity by ~45% is achieved at 323 K with a loading of 0.25 Vol% MAXene nanosheets. Interestingly, MAXene nanofluids exhibit decreased viscosity than the basefluid revealing that it can act as 'rheo-controlled' nanofluid. It is a unique rheological behavior, not exist in many well established conventional ceramic nanofluids. In addition, MAXene nanofluids also offer lubricating property with very low coefficient of friction (COF) values (<0.1).

1. Introduction

Heat transfer fluids exhibiting non-reactivity and exceptional thermal dissipation characteristics in addition to good thermo-chemical stability over a range of service temperatures have high demand in thermal management operations [1–3]. Practically, clogging in microchannels and poor fluid stability are the very common technical issues realized with classical thermal fluids prepared with conventional metallic particles [4–6]. This prompted researchers to develop 'nanofluids' using water [4] transformer oil [7], mineral oil [8], ethylene glycol [9,10], propylene glycol [11,12], silicone oil [13] basefluids dispersed with engineered particulates possessing high thermal conductivity. Factors affecting the bulk heat transfer in a thermal management fluid are dispersion stability, surface charge characteristics, fluid viscosity and

* Corresponding author. Tel.: +91 471 2515289, +91 9497271547.
E-mail address: ananthakumar70@gmail.com (S. Ananthakumar).

http://dx.doi.org/10.1016/j.cej.2016.04.010
1385-8947/

the morphology of nanoparticles. They are controlled by optimum use of particulate solid fraction, i.e., the filler fraction in the base-fluid [14]. Apart from the usual settling and choking problems, high filler loading increases viscosity and reduces the pumping efficiency, which is essential for mechanical circulation of the nano-fluid coolants. In fact, the viscosity of thermal fluids prepared with high thermal conducting Al_2O_3 [4], ZrO_2 [6], ZnO [12], Fe_2O_3 [15], SiC [16,17] and CeO_2 [18] etc. is quite high even at very low concentrations. Moreover, nano-particulates such as Al_2O_3, SiC and ZrO_2 dispersoids generate mechanical friction and associated frictional heat finally caused damage to mechanical components [19]. Therefore, a balance between thermal conductivity, stability and viscosity is imperative. It calls for new multifunctional nanostructures where desirable dispersion stability, viscosity and thermal conductivity can be reached.

Successive to many oxides, carbides, and nitrides dispersed ceramic thermal nanofluids, research was then shifted to carbon based nanofluids involving CNT nanostructures [20–22]. The very high thermal conductivity (2000–4000 W/mK) make it attractive for application in nanofluids. Unfortunately, in such nanofluids, the non-reactive CNT surfaces, intrinsic van der Waals force and geometrically high aspect ratios caused severe aggregation and make the system less stable. Surfactants were employed to overcome this drawback [23–25]. However, surfactant molecules cause foaming during heating and weaken the overall thermal properties. Moreover, the thermal resistance between CNTs and basefluid may increase due to surfactant molecules attached to the CNT surfaces [26]. Further, the entanglement and associated aggregation in CNT nanofluids causes an increase in viscosity and clogging in microchannels. To overcome this, Xie et al. introduced acid functionalization of CNTs to prepare surfactant free, stable CNT nanofluids [27]. Metal nanoparticle modification of CNTs is another method reported to improve the stability and performance of nanofluids [22].

2D nanostructures like graphene, fluorinated graphene oxide and boron nitride are recently emerged as potentially high thermal conducting, heat dissipative dispersoids in nanofluids to be used as nanocoolants [28–30]. Ramaprabhu and coworkers reported an enhancement of *ca.* 28% in thermal conductivity of water at 25 °C using metal oxide decorated graphene nanosheets [31]. A hybrid approach in which functionalized multiwalled CNTs are attached to functionalized graphene was also reported to prepare stable composite nanofluids with enhanced thermal properties [32]. Ajayan and coworkers explored BN nanosheets as electrically insulating thermal conductive fillers in transformer oil [33].

In this series, design of new 2D nanostructures is quickly growing. Recently our group reported the synthesis of a novel 2D nanostructure namely MAXene nanosheets from bulk Ti_3SiC_2 MAX phase ceramic nanolaminates for the first time [34]. MAX phase is the family of ternary carbides/nitrides denoted as $M_{n+1}AX_n$ where M is an early transition metal, A represents group IIIA, or IVA element and X is either carbon and/or nitrogen. It primarily consists of alternate MX layers separated by A layer atoms. Ti_3SiC_2 is the most familiar MAX phase studied extensively, including applications in structural composites [35–37]. Ti_3SiC_2 ternary carbides are novel engineering material possessing attractive functional properties. It is thermally stable like ceramics with exceptional machinability and thermal/electrical conductivity; features seen with metals. Bulk Ti_3SiC_2 has thermal conductivity in the range 37–40 W/mK [38]. Ti_3SiC_2 is also known for its self-lubricating properties [39]. Since Ti_3SiC_2 has unusual thermal, electrical and lubricating characteristics high interest is there to make multifunctional MAX phase nanostructures. We could produce 2D MAXene nanosheets via shear induced micromechanical delamination technique [34]. A few layers thick Ti_3SiC_2 MAXene nanosheets were found to be very well stable in polar solvents. Since these newly derived Ti_3SiC_2 MAXene nanosheets contain surface terminated hydroxyl groups, they are a promising candidate for obtaining water based thermal-fluids where high thermal conductivity, low viscosity and high lubricating properties can be expected.

Ethylene glycol and propylene glycol are two commonly used water- based fluid in thermal management. Even though ethylene glycol has better heat transport properties, propylene glycol is more non-toxic and environment-friendly than ethylene glycol [40,41]. The excellent antifreeze properties make propylene glycol based fluids one of the fastest growing product segment in heat transfer fluids. Thus, they are used as antifreeze agents in food and beverage industry [40]. Moreover, a liquid with a freezing point less than −40 °C is preferred for electronics cooling. Propylene glycol meets all these requirements. A summary of the demand for heat transfer fluids in the market is presented in Fig. 1. It can be seen that almost all the industries relevant sectors depend on heat transfer fluids to ensure reliable performance. Fig. 1(B) shows the market analysis of various kinds of heat transfer fluids in this decade. It is reported that the global market for all types of fluids is increasing year by year, which indicates the importance of developing new types of high performing fluids.

In the present study, we have successfully prepared a novel high thermal conducting Ti_3SiC_2 MAXene nanofluid in the propylene glycol medium. To the best of our knowledge, this is the first report demonstrating the application of 2D MAX phase nanosheets as heat carriers for heat transfer fluids. Interestingly, we also found unique rheological and lubricating properties in this newly designed MAXene thermal fluid. It is envisaged that the application of this multifunctional rheo-controlled 'MAXene nanocoolant' can contribute to the development of next generation heat transfer fluids.

2. Experimental

2.1. Materials and methods

Nanolayered Ti_3SiC_2 MAX phase (particle size Dav = 13 μm) was procured from 3-ONE-2 LLC, USA. Micromechanical milling was performed using the Ultra-Fine mortar grinder (Retsch-RM 200, Germany) which works on pressure–friction principle. Propylene glycol (Merck India Ltd) was used as the basefluid. An overview of the experimental procedure adopted in the present work is shown in Fig. 2. In a typical experiment 1 g of bulk Ti_3SiC_2 was taken in 15 mL propylene glycol. It was transferred into the ceramic Retsch mortar and subjected to micromechanical milling for 24 h. Before the last hour milling, the volume of propylene glycol was raised to 100 mL. After 24 h, the milled dispersion was transferred to a container and subjected to ultrasonication for 1 h using the ultrasonic processor (Sonics Vibra Cell, 20 kHz). The resultant dispersion was then centrifuged at 8000 rpm to settle down the un-exfoliated large particles. The delaminated Ti_3SiC_2 nanostructures stay suspended in the basefluid was collected for the preparation of nanofluid. The delaminated MAXene nanosheets required for morphological and structural characterization was collected by the removal of propylene glycol through solvent extraction method. For this, the nanofluid was diluted with an excess amount of chloroform and kept for few hours. The nanosheets settled at the bottom were collected by freeze drying. Conventional drying was avoided because it causes restacking of nanosheets. The separated nanosheets were preserved for further characterization. To prepare the nanofluids with various concentrations of Ti_3SiC_2 MAXenes, the solid content of the as processed dispersion was first determined gravimetrically by solid matter determination set up. For this thermal stability of the propylene glycol basefluid was first determined using thermogravimetric analysis (TGA) and it was found that

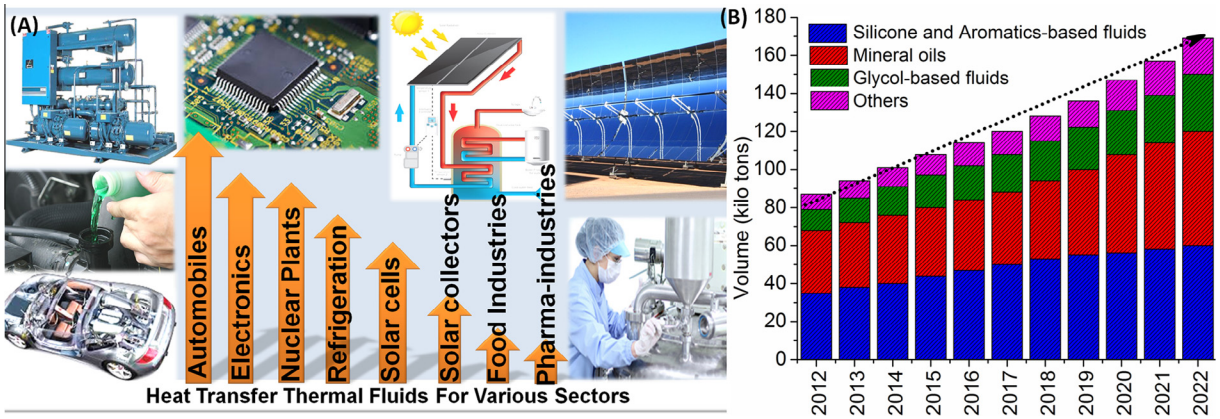

Fig. 1. (A) Insight on the usage of heat transfer thermal fluids in various industrial sectors. (B) Global market analysis of heat transfer thermal fluids by type with a forecast of the global consumption rate.

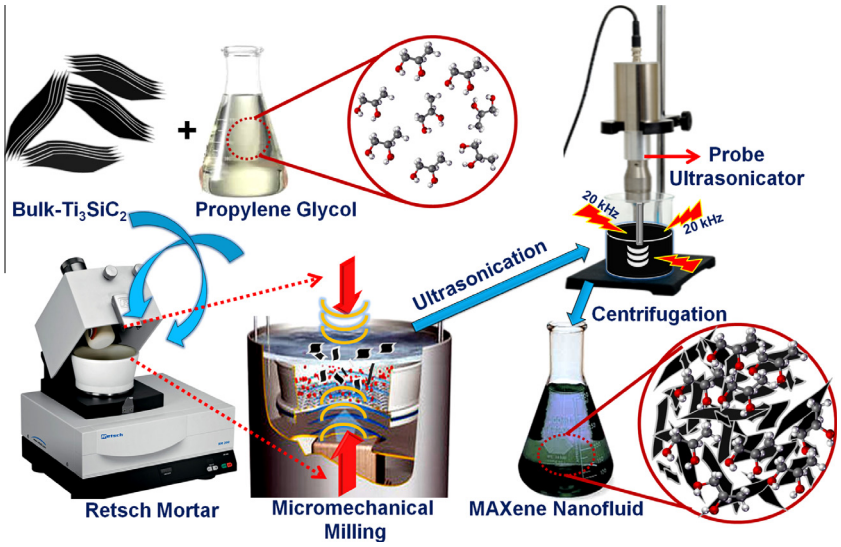

Fig. 2. Schematic representation of the processing of Ti_3SiC_2 MAXene nanofluids.

complete evaporation/decomposition of propylene glycol occurred at *ca.* 200 °C as shown Fig. S1 (Supporting Information). Hence, to determine the solid content, 10 mL of the as prepared nanofluid was taken in a clean, pre-weighed quartz crucible and then heated to 200 °C in a temperature controlled muffle furnace and kept at this temperature for 1 h. The weight of the crucible after cooling to room temperature was noted, and the solid concentration of the nanofluid was determined from the weight difference. The as prepared nanofluid was then diluted with sufficient amount of propylene glycol followed by 30 min ultrasonication to make homogeneous dispersions containing different volume concentrations of Ti_3SiC_2 MAXene nanosheets. The corresponding MAXene nanofluid is designated as PG-TSC-*x* Vol% (where, $x = 0.01$, 0.02, 0.1, 0.2 and 0.25).

2.2. Characterization

The microstructure of bulk Ti_3SiC_2 before exfoliation was analyzed using ZEISS EVO 18 Scanning Electron Microscopy (SEM). The morphological features of delaminated Ti_3SiC_2 MAXene sheets were examined by FEI Tecnai 30G2S-TWIN Transmission Electron Microscopy (TEM), operated at an accelerating voltage of 300 kV, coupled with EDX facility. The powder X-ray diffraction (XRD) pattern of the MAXene nanosheets was recorded using X'Pert Pro, Philips X-ray diffractometer with a monochromator on the diffraction beam side (Cu Kα radiation, $\lambda = 0.154$ nm). Size and zeta potential measurements for the nanofluids were conducted at 25 °C by Dynamic Light Scattering (DLS) using Malvern Zetasizer 3000HSA. The colloidal stability of the nanofluid was evaluated using Shimadzu UV-2401PC UV–vis Spectrophotometer. The rheological properties of the nanofluids were examined by Anton Paar Modular Compact Rheometer (MCR 102) using a measuring parallel plate setup (PP75) with 75 mm diameter and a gap of 1 mm. The rheo-experiments were conducted in flow (rotational) mode at a controlled rate with shear rates ranging from 0-1000S-1. The temperature dependent viscosity was measured in the temperature range 303–333 K at a constant shear rate of 200 S^{-1}.

The thermal conductivity of the nanofluid was recorded using KD2 Pro Thermal properties analyzer (Decagon Devices, USA) workings on the principle of transient hot-wire technique. The KS-1 probe having a diameter of 1.2 mm and a length of 6 cm was completely immersed in the nanofluid to determine the thermal conductivity. Typically the probe consists of a needle with a heater and a temperature sensor inside. A current passes through the heater and the system monitors the temperature of the sensor over time. Analysis of the sensor temperature determines the

thermal conductivity. Before the measurements, the probe was calibrated using standard fluid; glycerol supplied by KD2 Pro. Measurement of thermal conductivity of liquids is difficult and extreme care was taken to obtain accurate and repeatable results. The sample and the probe were kept absolutely still to eliminate any forced convection. The measurements were carried out in an isolated clean room that was free from any source of vibrations. The errors coming from convection mechanism were also reduced by aligning the sensor orientation in a vertical direction with the fluid container. Moreover, the high viscosity of propylene glycol than water minimizes the error due to convection. The temperature dependent measurements of thermal conductivity were carried out using a water bath. Thermal conductivity up to 323 K was measured since the viscosity becomes too low above this temperature and free convection begins to affect the measurement. A schematic representation of the experimental setup used for the thermal conductivity measurement is depicted in Fig. S2 (Supporting Information). The electrical conductivity of the nanofluids was measured using Jenway 3540 pH a Conductivity Meter with a cell constant of 1.02.

The tribological performance of the nanofluids was evaluated by ball-on-disc wear and friction technique (TR-201LE DUCOM, India). Steel balls (EN 31) having a diameter of 10 mm were used as standard test balls. A steel disc (EN 31 hardened to 62 HRc) having a diameter 100 mm and 8 mm thickness was used as the counterface material. A constant track diameter of 70 mm was given for all the measurements. The wear test was carried out with a normal load of 29.4 N and time of 900 s. The tests were conducted in an environmental chamber at ambient temperature. The nanofluid was applied on the wear track using a pump at a rate of 1 mL min^{-1}. A bare experiment was also conducted without the addition of any lubricants to determine the coefficient of friction of the steel ball. The frictional force was monitored by using a frictional force sensor and was converted to the coefficient of friction (μ). The surface roughness of the wear scar formed on the steel balls was measured using a surface roughness tester (Dektak XT Profilometer), with a measurement length of 0.8 mm.

3. Results and discussion

3.1. Preparation of MAXene nanofluids

The delamination of nanolayered, bulk MAX phase Ti_3SiC_2 particles into MAXene nanosheets and formation of nanofluids via mechanical shearing show a strong dependence on two processing parameters; milling time and initial mass. The gravimetric estimation of the solid fraction in the resultant MAXene nanofluids gives the % yield of the MAXene product at different processing conditions. Table 1 presents the effect of milling time and initial mass on the % yield of Ti_3SiC_2 MAXene nanosheets in a final volume of 100 mL propylene glycol. A maximum yield is obtained at a fixed time of 24 h milling for the initial feed of 1 g Ti_3SiC_2. It is seen that merely an increase in the initial mass of Ti_3SiC_2 feed could not improve the % yield though it is generally expected. Delamination of nanolayered Ti_3SiC_2 into MAXene nanosheets through mechanical means is possible by exfoliation, mechanical-peeling and thinning. In fact, factors such as inter-atomic bond strength, bulk hardness, and the dispersion stability of Ti_3SiC_2 in the given fluid medium are primarily controlled the effective mechanical exfoliation/delamination. Earlier reports on Ti_3SiC_2 clearly indicate that the TiC–Si bond is mechanically weak that can break and promote exfoliation/delamination when mechanical force is induced [42,43]. These reports confirm that the nanolaminated architectures can be mechanically separated from the original nanolayered stacked structure. We have earlier reported the effect of various solvents on the mechanical exfoliation/delamination of bulk Ti_3SiC_2 and found that polar solvents are effective in dispersion stability and rate of delamination [34].

Table 1
Dependence of initial Ti_3SiC_2 loading and milling time on % yield of MAXene nanosheets in the nanofluids.

Ti_3SiC_2 mass (g)	Milling time (h)	Solid fraction mg mL^{-1}	% yield
1	12	1.2	12
2	12	4.6	23
1	24	5.2	52
2	24	9.2	46
2.5	24	9.8	39
5	24	12.4	25

An operative mechanism in delamination of Ti_3SiC_2 is described schematically in Fig. 2. The delamination of the Ti_3SiC_2 particle in the propylene glycol medium is mainly aided by the oppositional rotation of mechanical mortar and the ceramic pestle coupled with the compressive shear force on the particles [34]. As the initial concentration increases, the particles move out from the contact area from the vicinity of the mortar and pestle of the Retch milling equipment and each particle is subjected to less milling process. As a result of this, the particle could not delaminate completely unless a proportional increase in the milling time is provided. This is the probable reason for the low yield even at high loading of Ti_3SiC_2. It was noticed that the centrifugation condition also influences the resultant yield of the MAXene product. We observed that the reduction of centrifugation time produced a dispersion of MAXene with a high % yield but with less stability. For example, at 4000 rpm/10 min duration, in addition to the colloidal size MAXene sheets, the centrifuged product also contains unexfoliated/partially exfoliated large and thick size MAXene sheets that make the dispersion less stable. At a given time of 24 h milling and 8000 rpm/10 min duration, the 1 g Ti_3SiC_2 feed produces completely exfoliated, stable MAXene nanofluid with 52% yield of solids. Therefore, these conditions were finalized to produce well stable MAXene nanofluids. Upon dilution with appropriate amounts of propylene glycol, MAXene nanofluids containing 0.01, 0.02, 0.1, 0.02 and 0.25 Vol% of Ti_3SiC_2 MAXene was successfully obtained.

3.2. Structural and morphological features of MAXene nanosheets

SEM and TEM examinations further ascertained the structural characteristics of the MAXene nanosheets formed via mechanical shearing and the resultant morphologies are depicted in Fig. 3. The schematic representation of layered arrangements of atoms in bulk Ti_3SiC_2 is given in Fig. 3(a). The SEM images in Fig. 3(b and c) show the nanolayered nature of bulk Ti_3SiC_2 particles that upon micromechanical exfoliation turn to MAXene nanosheets. The microstructure indicates the single Ti_3SiC_2 particle has a physical size below 10 μm. The particle also contains stacks of multiple nanothick inter-layers. Fig. 3(d1–d4) is the TEM morphologies of the exfoliated Ti_3SiC_2 MAXene nanosheets obtained in the propylene glycol medium. The TEM image describes three distinct nano morphologies of MAXene nanosheets in the nanofluids. In Fig 3 (d1) the TEM image shows a few layer thick, large size MAXene nanosheet with a sheet length of *ca.* 200 nm. A further examination reveals that the nanofluids also contain nanosheets with single layers and such layered sheets have the length of *ca.* 30–150 nm. These single layer MAXene sheets are transparent to electron beam as evidenced from HRTEM image in Fig. 3(d3). A low magnification TEM image and the corresponding statistical analysis illustrating the distribution of MAXene nanosheets in the nanofluid is given as Fig. S3 (Supporting Information). It is noticed that the nanofluid mainly contains nanosheets having length in the

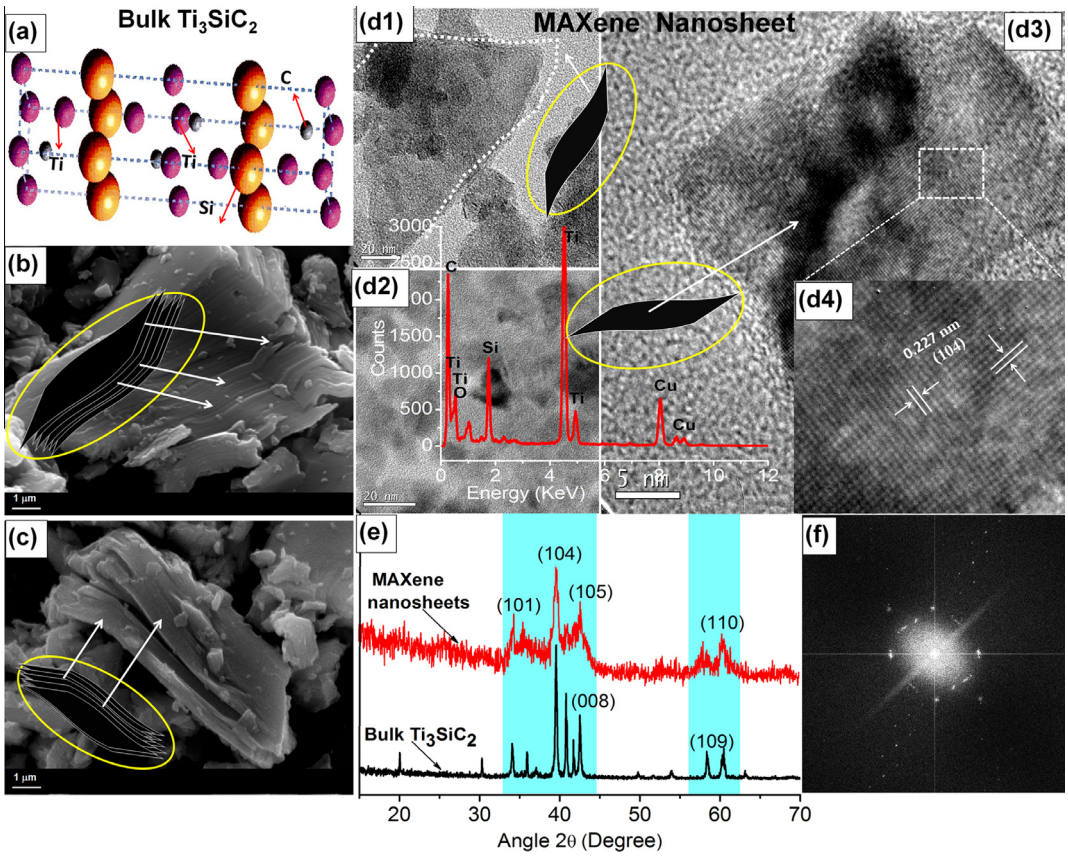

Fig. 3. (a) Schematic representation of crystal structure of bulk Ti_3SiC_2 revealing the layered arrangement of atoms, (b and c) SEM images of bulk Ti_3SiC_2 showing the nanolayered characteristics, d1–d3) TEM images of Ti_3SiC_2 MAXene nanosheets showing various size distribution in the nanofluids, The inset to the TEM image represents the corresponding EDX spectrum, (d4) magnified portion of HRTEM image of single MAXene nanosheets shown in d3, (e) the powder XRD spectra of bulk as well as exfoliated MAXene nanosheets and (f) FFT corresponds to the TEM images shown in d3.

range 30–150 nm. The inset to Fig. 3(d3) is the magnified part of the single nanosheet revealing the orientation in (1 0 4) plane with a d spacing of 0.227 nm. The corresponding FFT pattern is also depicted in Fig. 3(f). In addition to these large size thick and single layer Ti_3SiC_2 MAXene nanosheets, the micro-mechanical exfoliation of bulk Ti_3SiC_2 also produced a significant amount of ultra-small Ti_3SiC_2 quantum dots with size *ca.*10 nm as seen in Fig. 3 (d2). The parallel existence of Ti_3SiC_2 quantum dots is the result of the micromechanical grinding effect due to an extended period of mechanical shearing where the destruction of Ti_3SiC_2 readily occurred. Such mixed morphologies of nanosheets with different sheet lengths and nanoparticles are expected to offer increased inter-particle contacts and maintain the particle networking to have effective thermal transport. The EDX spectrum of the MAXene nanosheets is given as inset to the TEM images (Fig. 3d1–d4). The presence of OH functionalities on the surface of the MAXene nanosheets is distinguished in the spectrum. Formation of the surface oxygen group is due to the micro-thermal heat produced during mechanical milling in the polar solvent for long hours. The electrostatic interaction of these OH groups with the propylene glycol leads to the formation of very stable dispersions without any settling. The phase purity and crystallinity of MAXene nanosheets can be understood from the corresponding powder X-ray diffraction patterns given in Fig. 3(e). The XRD pattern of the bulk Ti_3SiC_2 was also presented to verify the crystal features of MAXene nanosheets. It is observed that the nanosheets retain its chemical identity, and the results are on par with the earlier reports [34]. As expected the nanosheets have highly broadened crystalline peaks and in such nanoscale, the peak intensity largely decreased. From the XRD, it is confirmed that the mechanically delaminated MAXene layers preferably have few layer thick ultra-thin dimensions. In fact the higher order peaks seen in bulk Ti_3SiC_2 is absent in the XRD spectrum of MAXene nanosheets confirming its 2D characteristics.

Fig. 4 represents the physical stability of the MAXene nanosheets in propylene glycol based fluids with different concentrations. Normally the main challenge in obtaining a highly thermal conducting nanofluid is the dispersion and stabilization of nanoparticles. In many cases, nanoscale dispersoids easily stay dispersed at low concentrations. However, for effective thermal transport, a high solid fraction is important and at high solid concentrations, the dispersion stability is very poor. The addition of suitable surfactants is usually employed to overcome this problem. But unfortunately, the surfactants affect the bulk thermal transport characteristics. Here, the MAXene nanosheets form a very stable dispersion in propylene glycol even at high concentrations without the aid of any surfactants or stabilizers. Fig. 4 shows the stability of MAXene nanofluids in comparison with the nanofluid prepared with unexfoliated bulk Ti_3SiC_2. Fig. 4(A) corresponds to the physical stability of 0.1 Vol% bulk Ti_3SiC_2 nanofluid processed by ultrasonication only. In propylene glycol, the bulk particles form dispersion, but they started settling immediately after preparation and completely settled in 3 days of period. The density of the Ti_3SiC_2 is 4.53 g cm^{-3}. The propylene glycol density and theoretical viscosity are 1.04 g cm^{-3} and 0.42 cPa s, respectively. The bulk Ti_3SiC_2 used in the present study has an average particle size of 13 μm. The high density and particle size make it difficult to disperse it in the reasonably viscous glycol medium even at low

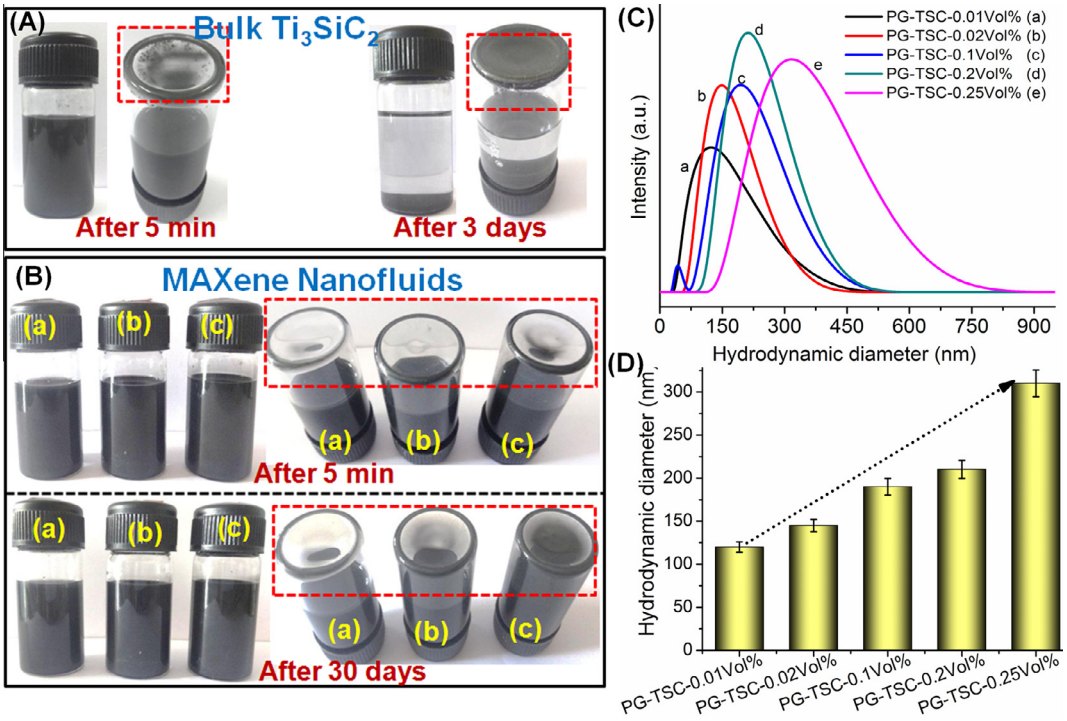

Fig. 4. Photographs showing the dispersion stability of the MAXene nanofluids prepared with (A) bulk Ti_3SiC_2 and (B) Ti_3SiC_2 MAXene nanosheets; (a) PG-TSC-0.01 Vol%, (b) PG-TSC-0.2 Vol% and (c) PG-TSC-0.25 Vol%. Variation in the hydrodynamic diameter of the nanofluids as a function of MAXene loading in the nanofluids is shown in C and D.

solid loading. However, in the case of MAXene nanosheets, the nanofluids offer high stability even after keeping undisturbed for more than a month (Fig. 4B). The stability is not affected by the increase in the solid loading. It was observed that the cold pressed 2D MAXene nanosheets derived from the bulk Ti_3SiC_2 possess low density of ~1.45 g cm^{-3} only (determined from physical dimensions and weight). Apart from the nanoscale dimensions, as evidenced by the EDX analysis, the presence of chemically interactive surface functional moieties favoring the high colloidal stability in MAXene nanofluids. When solids loading have gradually increased the tendency of interparticle aggregation is seen. Nevertheless, the aggregates exhibit good stability up to the solids loading of 0.2 Vol% MAXene. Above this range, a minimal settling was observed. However, it was observed that the sediment formed is reversible and a simple hand shaking is enough to make it again a stable dispersion.

The stability of the nanofluid is also analyzed using UV–vis spectroscopy studies and the results are depicted as Figs. S4 and S5 (Supporting Information). UV–vis spectroscopy is a common tool for the sedimentation characteristics analysis of nanoparticles in a dispersion and evaluate the stability of nanofluids [44]. According to Beer–Lambert law, the absorbance of a solution is directly proportional to the concentration of the absorbing species such as particles in a dispersion and therefore this method is a unique technique to determine the particle concentration in a dispersion. It is observed that the dispersions are well stable even after kept undisturbed for more than 1 month. Only about 13% sedimentation is seen in the case of the highest concentration (0.25 Vol%). The sedimentation is negligible in the case of lower concentrations. We also checked the zeta potential values to validate the colloidal stability of MAXene nanofluids. It is seen the zeta potential value is increased from −24.1 to −38 mV when the amount of MAXene nanosheets is increased from 0.01 to 0.25 Vol %. The relatively high zeta potential value confirms the colloidal stability.

To get an insight of the particle–solvent interaction, the hydrodynamic diameter of the MAXene nanosheets with respect to their concentration in propylene glycol was monitored using DLS measurements and the size distribution result is shown in Fig. 4(C and D). In DLS technique for non-spherical particles, the size is interpreted as an equivalent spherical diameter equal to Stokes–Einstein hydrodynamic diameter. The hydrodynamic diameter includes both the inorganic core as well as the attached solvent layer. It was observed that the average hydrodynamic diameter increased from 120 to 310 nm with respect to the increase in MAXene loading from 0.01 Vol% to 0.25 Vol%. The increase in the hydrodynamic diameter indirectly indicates the strong interaction of the MAXene nanosheets with the dispersion medium. The high hydrodynamic diameter observed in the present case suggests a strong hydrophilic interaction between propylene glycol medium and MAXene nanosheets. It is interesting to note that unlike many 2D nanostructures, the MAXene nanosheets have advantages in two ways; it works well with mechanical dispersion technique, it produces dimensionally varying mixed morphologies and finally high stability at high solid concentrations even in the absence of any surfactants. All these make it potential for the processing of multifunctional MAXene 'nanocoolant'.

3.3. MAXene nanocoolant performance – rheological properties

Viscosity is very critical for a thermal fluid because mostly the thermal fluids are used under continuous flow applications. The flow characteristics of basefluid should not be increased when the active nanofillers are introduced. Earlier studies on the viscosity of nanofluids prepared with conventional metallic and ceramic nanoparticles for thermal management operations strongly indicate an increase in the viscosity with increasing nanofiller addition [6,18]. The aggregation effect and weak interactive surface forces with the fluid medium were said to be the reasons for the abrupt rise in the viscosity. In a shear flow, the hydrodynamic forces

required to break the network of aggregated nanoparticles into individual primary nanoparticles are insufficient. This causes an increase in viscosity of the system than that of the basefluid. Usually, a well dispersed nanofluid exhibit lower viscosity than that of a less stable, aggregated dispersion with equivalent solid loading and several reports documented the need of steric or electrostatic stabilization techniques to control the aggregation effect and minimize the increase in viscosity [45,46]. The rheology of MAXene nanofluids developed in the present work was evaluated using cone and plate rheometer. The variation of room temperature viscosity with the shear rate ranging between 0 and 1000 s^{-1} was investigated with respect to MAXene loading, and the results are given in Fig. 5. The flow curves clearly explain that the viscosity of the MAXene nanofluid is independent of shear rate and is following the Newtonian flow behavior. The shear stress curves also follow the same patterns (Fig. 5b). This indicates that even though the inter-particle clustering occurs, they are feeble in nature that gets separated easily under applied mechanical stress. In MAXene nanofluid, the interesting factor to be noticed is that the remarkable decrease in the viscosity values. The flow curve corresponds to the propylene glycol basefluid shows the value ~38 mPa s. The intermolecular hydrogen bonding between the molecular chains is responsible for the viscosity of propylene. The viscosity value gradually decreases with the loading of MAXene up to 0.2 Vol%. Beyond this range, the viscosity appears to increase. However, the viscosity value is still well below that of the basefluid. The flow-property results confirm the good interfacial interaction among the nanosheets with the basefluid. Propylene glycol have chemically weak hydrogen bonding and due to the interfacial interaction with MAXene nanosheets, the weakening of hydrogen bonds happens and finally resulted in dropping of the fluid viscosity. The interfacial interaction is mainly governed by the hydrophilic surface functional groups present in the nanosheets. The surface hydroxyl groups present on MAXene nanostructure bridge with hydroxyl groups in the propylene glycol that possibly form weak hydrogen bonds and decreases the fluid viscosity. Tan et al. reported the formation of such kind of interactions in reduced graphene oxide dispersion in polyvinyl alcohol [47]. The reduction in viscosity with MAXene loading may be due to mainly by three factors; (1) at very low concentrations of nanosheets, the like charges repel each other and reduce the inter-particle interactions that in turn prevent associated increase in viscosity (2) the hydrophilic MAXene nanosheets can easily bond with hydroxyl groups of propylene glycol and thereby decrease the interaction between the fluid molecular chains and causes lowering of viscosity and (3) the nanosheets can easily align themselves in the direction of shear force and act as lubricant materials and reduce the friction (between the particles as well as the fluid and the walls of the container) which will eventually result in a sharp decrease in viscosity and allows smooth flow of the fluids.

Fig. 6 shows the temperature dependent rheological behavior of the MAXene nanofluids evaluated in the range 303–333 K at a constant shear rate of 200 s^{-1}. The flow curves confirm a decrease in viscosity with increasing temperatures in both basefluid as well as MAXene nanofluid. The propylene glycol viscosity decreases sharply from the value of 38 to 8 mPa s at 333 K. The nanofluids containing MAXene nanosheets also follow the same trend. Fig. 6 (b) represents the relative viscosity (μ_r) of the nanofluids with respect to the basefluid calculated using the expression;

$$\mu_r = \mu_{nf}/\mu_b \quad (1)$$

where μ_{nf} and μ_b are the viscosities of nanofluid and the basefluid, respectively. In many nanofluid systems reported earlier, the viscosity of the nanofluid is greater than that of the basefluid and hence, the relative viscosity is always higher than the parent fluid used for the preparation of nanofluid. However, in this present work, a unique performance of MAXene nanofluid was observed. The results on the relative viscosities of the MAXene nanofluids confirm that the relative viscosity is <1 at all the concentrations in the entire temperature range of 303–333 K. The relative viscosity of MAXene nanofluid prepared with 0.2 Vol% concentration is only about 0.70 at room temperature, which accounts for a reduction of 30% in the viscosity compared to the basefluid. Such a substantial reduction in viscosity gives a great advantage in improved pumpability (easiness of pumping) and high thermal conductivity in the MAXene nanofluid. It is clear from the Fig. 6b that the relative viscosity is very less at low temperatures. At elevated temperatures, the relative viscosity is gradually increased. However, the value is still <1.

3.4. Thermal conductivity performance of MAXene nanocoolants

The trend in the thermal conductivity enhancement of the MAXene nanofluids with different MAXene concentrations is presented in Fig. 7. The enhancement in the thermal conductivity was computed from the equation;

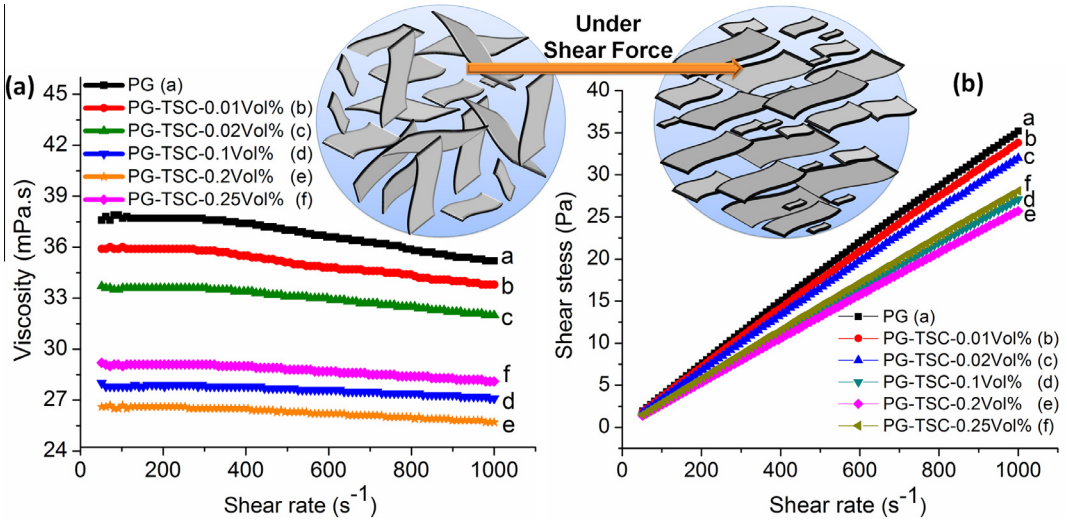

Fig. 5. Rheological properties of the nanofluids (a) variation in viscosity with shear rate and (b) variation of shear stress with shear rate. Schematic representation showing the easy flow behavior of nanofluids under shear force is given as inset.

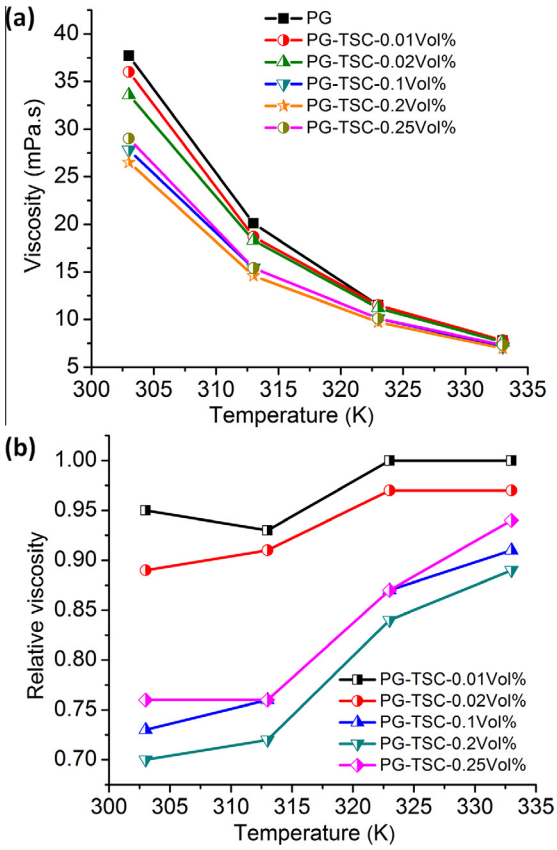

Fig. 6. Dependence of (a) viscosity and (b) relative viscosity on temperature.

$$K_{\text{eff}} = (k_{nf} - k_0)/k_0 \times 100 \quad (2)$$

where k_{nf} and k_0 are the thermal conductivities of MAXene nanofluid and propylene glycol basefluid, respectively. Fig. 7(a) illustrates the concentration dependent thermal conductivity of MAXene nanofluid at two different temperatures, 303 K (30 °C) and 323 K (50 °C). It is observed that at both the temperatures, MAXene nanofluids show an increased thermal conductivity with increasing concentration of MAXene nano dispersoids. The thermal conductivity enhancement is almost linear with an increase in the MAXene loading. It is noticed that at the given experimental temperatures of 303 K and 323 K, the thermal conductivity enhancement is apparently significant and the percentage increase achieved is approximately 45% when the MAXene concentration, as well as the applied temperatures, are at their maximum. More specifically, at 303 K, the MAXene concentration of 0.01 Vol% accounts only 5% in thermal conductivity which is increased to 15% when the MAXene loading is increased to 0.25 Vol%. At this identical concentration level, the thermal conductivity enhancement at an elevated temperature of 323 K is ~45%.

Fig. 7(b) describes the influence of temperatures on the enhancement in thermal conductivity of MAXene nanofluids processed at different concentrations. The corresponding thermal conductivity data of the basefluid and MAXene nanofluids are given in Fig. S6 (Supporting Information) for clearer understanding. As expected, in the absence of any active MAXene nanofillers, the thermal conductivity of propylene glycol does not show any dependence on temperature and retain almost a constant value, ~0.191 W/m K in the whole temperature ranges. However, upon dispersion of MAXene nanosheets, the nanofluids show a prominent increase in the thermal conductivity with increasing applied temperatures. For example, when the propylene glycol is loaded with 0.25 Vol% of MAXene fillers, the thermal conductivity is increased from 0.191 to 0.276 W/m K at 323 K. This confirms that the MAXene nanofillers play a key role in thermal transport of the bulk nanofluid. More accurate measurements of thermal conductivity were hard to observe beyond 323 K and the values were fluctuating due to free convection at higher temperatures. It results in statistically large errors and, therefore, could not be included here. The increase in the effective thermal conductivity (k_{eff}) with temperature is a result of Brownian motion in the MAXene nano colloid and is in accordance with predictions of Maxwell [15,33].

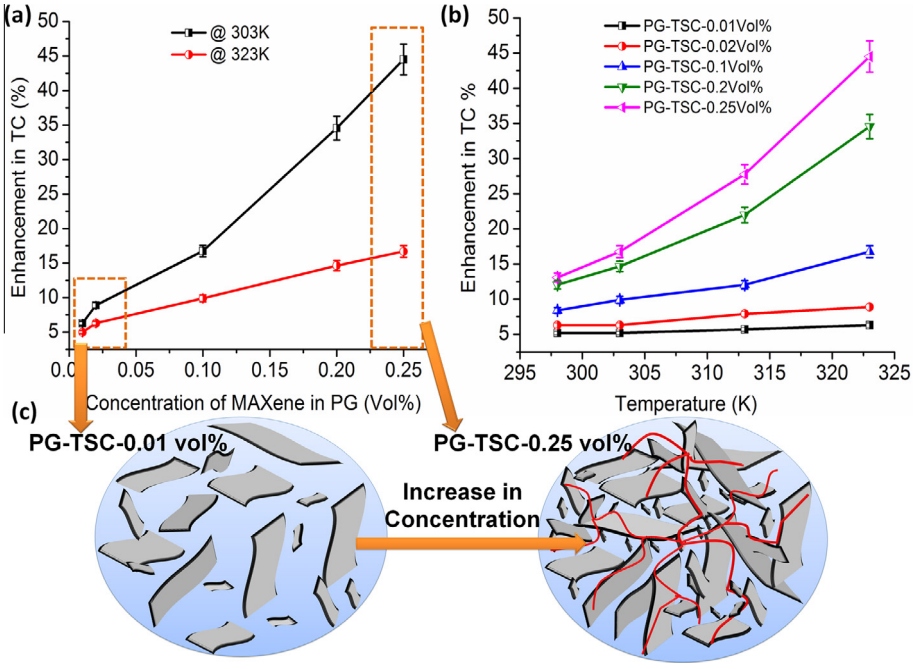

Fig. 7. Variation of thermal conductivities of the nanofluids with (a) concentration and (b) temperature. (c) Schematic representation of the role of Ti_3SiC_2 MAXene concentration on thermal conductivity.

As we discussed earlier, the hydrophilic nature of MAXenes provide good interaction with the basefluid and form effective liquid layering at MAXene-propylene glycol interface. The drastic decrease in the viscosity of propylene glycol in the presence of MAXene nanodispersoids is in fact, supporting the liquid layering effect. The liquid layering as well as the lowering of viscosity are the factors governing the improvement in the bulk thermal conductivity of the basefluid [11,12]. The low viscosity possibly promotes the particle movement in the fluid much easier and makes them as effective carriers of heat energy. One essential difference in this work to be worth indicating is that the MAXene nanosheets are dispersed in propylene glycol without the use of any surfactants or stabilizing agents. This adds advantage of this present nanofluid design. Earlier studies confirmed that the surfactant layers reduced the thermal conductivity owing to defects created by them, which ultimately retard the free electron/phonon transportation. So surfactants free nanofluids, such as the one reported in his work, are always attractive for the sustainable thermal transport and thermal management applications.

The increase in thermal conductivity with increasing filler content suggests further that the percolation mechanism also significantly contributes to the thermal transport. This indicates that Maxwell's theory is not following at high filler concentrations. According to Maxwell's theory concentration have very small impact on thermal conductivity. We have earlier confirmed from the TEM images that the MAXene nanosheets in propylene glycol nanofluids exhibit morphologically varied nanostructures with varying dimensions. Such mixed morphologies can effectively maintain the percolative channel for maximizing the thermal transport at higher filler loading as shown schematically in Fig. 7 (C). Over the period, we also observed a weak clustering of the MAXene nanosheets as claimed from the marginal increase in the hydrodynamic particle size data. This clustering effect is in fact, one among many reasons reported earlier for the improvement in the thermal conductivity of nanofluids. Fig. 8 depicts the increase in thermal conductivity with the hydrodynamic diameter of the MAXene nanofluid. It is clear that the thermal conductivity is increasing with the increase in the hydrodynamic size. The increase is more prominent at high temperatures due to the additive effect of both Brownian motion and percolation mechanism.

3.5. Efficiency of the nanofluids

The performance of nanofluids also depends on the flow mode (laminar/turbulent) and in the case of laminar flow, for an ideal nanofluid; the ratio of viscous to thermal conductivity coefficients should be < 4 i.e. the increase in the viscosity is less than four times the increase in thermal conductivity [6,48]. This is usually estimated using the dynamics relations by the equations;

$$\eta_{nf}/\eta_{bf} = 1 + C_\eta \quad (3)$$

$$K_{nf}/k_{bf} = 1 + C_k \quad (4)$$

$$C_\eta/C_k < 4 \quad (5)$$

where η_{nf}/η_{bf} and k_{nf}/k_{bf} are respectively the ratios of experimental viscosity and thermal conductivity of nanofluids with the basefluid. C_η and C_k are the viscosity and thermal conductivity enhancement coefficients. The C_η/C_k values calculated for the MAXene nanofluids at temperatures 303 K and 323 K are given in Table 2. Usually, the addition of ceramic and metallic nanofillers in basefluids resulted in an increase in viscosity and therefore, C_η/C_k is always positive. In this MAXene nanofluid design, it can be understood from tabulated values, the ratio of viscosity and thermal conductivity enhancement coefficients is much lower than the critical limit of 4. In all concentrations (0.01–0.25. Vol%) of Ti_3SiC_2 MAXene nanosheets, the C_η/C_k values are not only lower than zero but also they fall in the negative range. The negative value is a result of the decreased viscosity of MAXene nanofluids with MAXene dispersoids. A performance comparison of rheological and thermal properties of MAXene nanofluid with other nanofluids reported in the literature is given as Table S1 (Supporting Information). It can be understood that 2D nanosheets such as born nitride and graphene is reported the maximum enhancement in thermal conductivity. However, their performance is limited by the unfavorable increase in viscosity. In the case of MAXene nanofluid, the viscosity is reduced by 30% compared to the basefluid along with comparatively higher enhancement in thermal conductivity. Both these properties make it an excellent nanocoolant.

3.6. Lubricating performance of the nanofluids

The lubrication effect by the well dispersed MAXene nanofluid is studied by ball on disc wear and friction technique, and the results are presented in Fig. 9. In fact, in most of the earlier works, attempts were made only to report the thermal properties. Their tribological performance is seldom reported. The lubricating effect of the nanofluids is also significant like thermal conductivity since high friction, heat generation, increased viscosity and high wear are interrelated factors for deteriorating the performance of any structural component in a typical mechanical operation. From Fig. 9(a) it is seen that the frictional force is largely decreased when the MAXene functional nanofluid is introduced in the wear track. The bare steel ball is exerting a high frictional force against the steel disc in the absence of any MAXene nano lubricant. The frictional force falls, approximately 4 times compared to the bare steel ball when the MAXene nanofluids are introduced. It is known that the propylene glycol basefluid possesses a considerable lubrication property. However, when the addition of conventional ceramic nanofillers with this basefluid is employed, it causes an increase

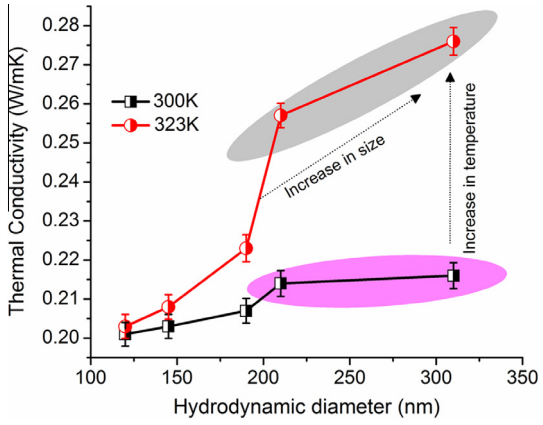

Fig. 8. The dependence of thermal conductivity with the hydrodynamic diameter of the MAXene nanosheets at temperatures of 300 K and 323 K.

Table 2
Ratio of viscosity and thermal conductivity enhancement coefficients as a function of Vol% of MAXenes at two different temperatures.

Sample	C_η/C_k	
	303 K	323 K
PG-TSC-0.01 Vol%	−0.86	−0.17
PG-TSC-0.02 Vol%	−1.73	−0.34
PG-TSC-0.1 Vol%	−2.64	−0.78
PG-TSC-0.2 Vol%	−2.03	−0.47
PG-TSC-0.25 Vol%	−1.38	−0.28

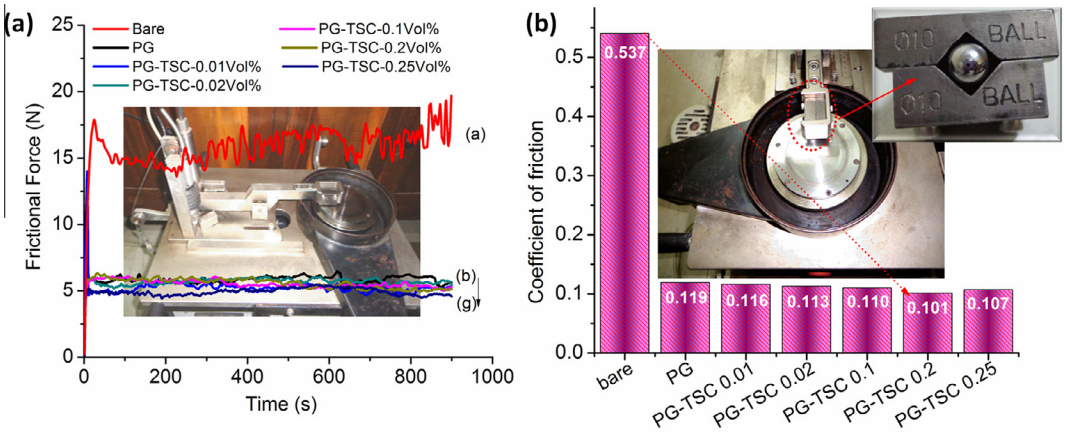

Fig. 9. The tribological performance of the MAXene nanofluids (a) frictional force and (b) coefficient of friction with respect to different Ti_3SiC_2 MAXene loading.

in the fluid viscosity that deteriorates its inherent lubricating property. In spite of the increase in the thermal transport in a typical ceramic nanofluid, such a loss in the lubricating property due to the relatively high hardness of the ceramic nanomaterial and high viscosity of ceramic nanofluids makes most of the nanofluids unsuitable for the thermal fluid applications [19]. Surprisingly, the addition of Ti_3SiC_2 MAXene nanosheets does not seem to affect the lubricating characteristics of the basefluid, propylene glycol. MAX phase materials are already known to exhibit self-lubricating nature [39]. Several ceramic and polymer composites showed low coefficient of friction and excellent wear resistance than the matrix when Ti_3SiC_2 was used as active filler [34,49]. With this lubricating effect of propylene glycol-MAXene nanodispersion, the nanofluid not only tender the thermal management function but also retain the minimum frictional force and thereby avoid the heat generation and wearing of the structural parts.

Fig. 9(b) demonstrates the decrease in the coefficient of friction (COF) values when the MAXene lubricating nano fluid is applied to the contact point between the ball and disc. When polypropylene glycol is introduced without any MAXene nanolubricant, the COF value decreased from 0.54 to 0.12. When nanofluid containing 0.2 Vol% MAXene nanosheets is employed, the coefficient of friction value decreases to a lower value of 0.1. It is worth noticing that the wear resistance is largely improved in the presence of MAXene nanofluids. The optical microscopic images of the steel balls after wear tests at various conditions are given in Fig. 10 which indirectly indicates the lubricating action of the MAXene nanocoolant. It is observed that in the absence of MAXene nano lubricant, the surface of the test specimen reveals a strong and deep wear scar in the diameter of ~1450 μm. This was reduced to ~750 μm when propylene glycol is added without MAXene nanosheets. The wear diameter further decreased 670 μm at 0.2 Vol% additions of MAXene nanosheets indicating the layered MAXene nanostructures offer lubricating effect and improve the wear resistance. The roughness of wear tracks were analyzed by surface profilometry. The corresponding profilometer curves showing the hills and valleys on the wear scar are given in Fig. 11. It is seen that depth of the valleys and the height of the hills are more prominent in the absence of nanofluids. The surface appears smooth when the MAXene nanofluid is used. The wear scars on steel ball under no lubrication condition have a surface roughness of 765 nm. The value is estimated as 215 nm when propylene glycol is used. The surface roughness further decreasing when nanofluid containing MAXene nanosheets is used. The wear scar of the steel balls with 0.1 and 0.2 Vol% MAXene nanosheets possess reduced roughness of 125 and 138 nm, respectively. All these observations reveal that the nanofluid developed in the present work is acting as a multifunctional nanofluid with controlled rheological performance, enhanced thermal transport properties, and improved lubrication properties.

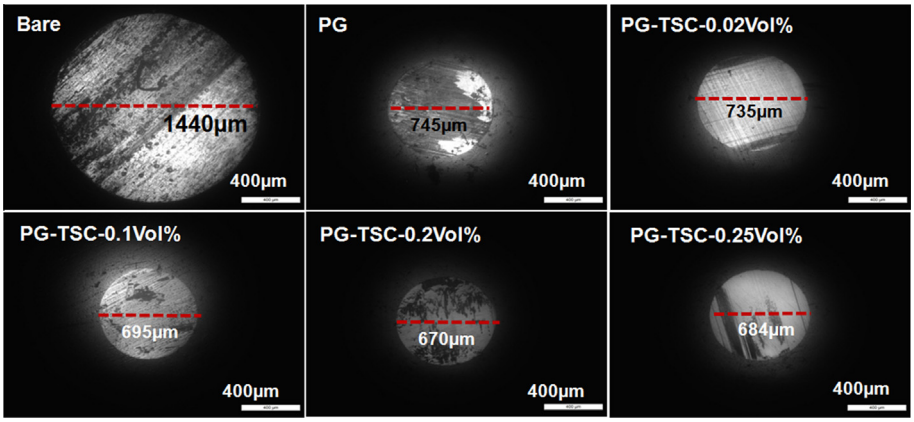

Fig. 10. The optical microscopic images of the wear scar formed on the steel ball at different experimental conditions. The wear diameter in each case is marked as a red line. (For interpretation of the references to color in this figure legend, the reader is referred to the web version of this article.)

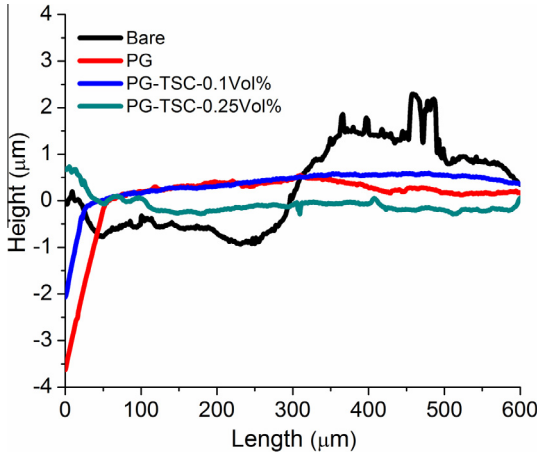

Fig. 11. The Surface profilometer curves of the steel balls at different lubrication conditions.

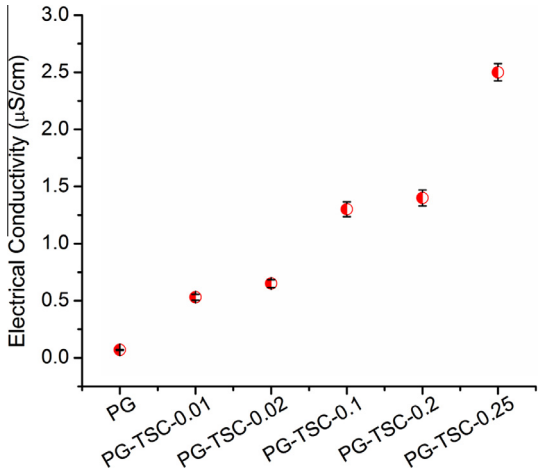

Fig. 12. The electrical conductivity of the MAXene nanofluids at room temperature as a function of MAXene loading.

3.7. Electrical properties of the nanofluids

The electrical conductivity of the nanofluid is also important since some applications required fluids with least electrical conductivity. The electrical conductivity of the nanofluids with respect to MAXene concentration was measured at room temperature, and the results are presented in Fig. 12. The electrical conductivity of the nanofluid is increasing with an increase in the amount of MAXene nanosheets. The basefluid, propylene glycol exhibits an electrical conductivity of <0.1 μS cm^{-1} which is increased to 2.5 μS cm^{-1} when the MAXene content in the fluid increased to 0.25 Vol%. Since the volume fraction of the MAXene nanomaterial in the nanofluids is less, there is no abrupt increase seen in the electrical conductivity. The electrical conductivity increase in MAXene nanofluid is negligible when compared with graphene oxide based nanofluids [30].

4. Conclusions

In this work, a new nanofluid is designed and systematically investigated for its promising beneficial properties. In situ processing of Ti_3SiC_2 MAXene nanosheets in propylene glycol medium via shear induced micromechanical cleavage technique resulted in highly stable surfactant-free thermal nanofluid. This new nanofluid qualifies all the necessary requirements for a heat-transport thermal management fluid. The salient features of the Ti_3SiC_2 MAXene nanofluids processed in this work are:

1. The shear-induced micromechanical cleavage technique successfully resulted in mixed morphologies of MAXene nanostructures consist of 10 nm size MAXene dots and 30–200 nm sized 2D-nanosheets with the surface associated OH-functional groups that eventually retain the colloidal stability.
2. The rheology study confirms that the MAXene dispersed polypropylene glycol nanofluid attains unusually decreased viscosity even when the solid fraction of MAXene is increased. At a concentration of 0.2 Vol%, MAXene dispersion showed 30% reduction in viscosity. The shear rate v/s viscosity flow curves strongly suggest that the nanofluid obeys Newtonian flow behavior. Such a control over viscosity favorably increases the pumpabilty (easiness of pumping) of MAXene nanofluid that is necessary for ideal circulation during cooling operations.
3. The thermal property studies strongly indicate the nanolayered; mixed morphologies of stable MAXene nanostructures significantly increase the bulk thermal conductivity due to percolation mechanism. The nanofluid prepared with 0.25 Vol% of MAXene dispersoids showed a 15% increase thermal conductivity at room temperature, which was further enhanced to 45% at a temperature of 323 K.
4. Interestingly, the MAXene-propylene glycol nanofluids offer a lubrication property that was confirmed by ball-on-disc wear and friction test. Under dry friction test condition, a coefficient of friction value 0.54 was seen which decreased to 0.1 when the fluid containing 0.2 Vol% MAXene dispersion was employed. The self-lubricating property of MAXene nanosheets and reduced viscosity are the key players in this phenomenon. Such lubrication effect decreases the wearing of structural parts and thereby improves the efficiency when it is subjected to an actual application.

Ultimately the study reveals that the MAXene nanofluid is an all-rounder with multifunctionalities with respect to rheo-control, thermal conductivity and lubrication property that make the system an effective nanocoolant for thermal management applications.

Acknowledgements

The authors are thankful to the Director, CSIR-National Institute for Interdisciplinary Science and Technology for providing the necessary lab facilities. The authors are grateful to Mr. Kiran Mohan for TEM analysis and Mr. V.R. Rajeev for Profilometer measurements. K.V.M. acknowledges Council of Scientific and Industrial Research (CSIR), Govt. of India for Senior Research Fellowship.

Appendix A. Supplementary data

Supplementary data associated with this article can be found, in the online version, at http://dx.doi.org/10.1016/j.cej.2016.04.010.

References

[1] C.Y. Zhi, Y.B. Xu, Y. Bando, D. Golberg, Highly thermo-conductive fluid with boron nitride nanofillers, ACS Nano 5 (2011) 6571–6577.
[2] W. Yu, H.Q. Xie, D. Bao, Enhanced thermal conductivities of nanofluids containing graphene oxide nanosheets, Nanotechnology 21 (2010) 1–7.
[3] K. Dey, D. Bhatnagar, A. Srivastava, M. Wan, S. Singh, R. Yadav, B. Yadav, M. Deepa, VO_2 nanorods for efficient performance in thermal fluids and sensors, Nanoscale 7 (2015) 6159–6172.
[4] H. Jonggan, K. Dongsik, Effects of aggregation on the thermal conductivity of alumina/water nanofluids, thermochim, Acta 542 (2012) 28–32.

[5] G. Prasad, S.S. Naik, A. Komel, S. Srinath, K.A. Kishore, Y.P. Setty, S. Shirish, Stable colloidal copper nanoparticles for a nanofluid: production and application, Colloids Surf. A 441 (2014) 589–597.

[6] T.S. Sreeremya, K. Asha, L.N. Satapathy, S. Ghosh, Facile synthetic strategy of oleophilic zirconia nanoparticles allows preparation of highly stable thermo-conductive coolant, RSC Adv. 4 (2014) 28020–28028.

[7] C. Choi, H.S. Yoo, J.M. Oh, Preparation and heat transfer properties of nanoparticle intransformer oil dispersions as advanced energy-efficient coolants, Curr. Appl. Phys. 8 (2008) 710–712.

[8] T.-T. Jose Jaime, N.T. Narayanan, T. Chandra Sekhar, L. Karen, C. Mircea, P.M. Ajayan, Nanodiamond-based thermal fluids, ACS Appl. Mater. Interfaces 6 (2014) 4778–4785.

[9] V. Kumaresan, R. Velraj, Experimental investigation of the thermo-physical properties of water–ethylene glycol mixture based CNT nanofluids, Thermochim. Acta 545 (2012) 180–186.

[10] M.C.S. Reddy, V.V. Rao, Experimental studies on thermal conductivity of blends of ethylene glycol–water-based TiO_2 nanofluids, Int. Commun. Heat Mass Transfer 46 (2013) 31–36.

[11] S. Manikandan, K.S. Rajan, Rapid synthesis of MgO nanoparticles & their utilization for formulation of a propylene glycol based nanofluid with superior transport properties, RSC Adv. 4 (2014) 51830–51837.

[12] K.S. Suganthi, M. Parthasarathy, K.S. Rajan, Liquid-layering induced, temperature-dependent thermal conductivity enhancement in ZnO–propylene glycol nanofluids, Chem. Phys. Lett. 561–562 (2013) 120–124.

[13] C. Lifei, X. Huaqing, Silicon oil based multiwalled carbon nanotubes nanofluid with optimized thermal conductivity enhancement, Colloids Surf. A 352 (2009) 136–140.

[14] S.U.S. Choi, Nanofluids: from vision to reality through research, J. Heat Transfer 131 (2009) 033106–033109.

[15] P.D. Shima, P. John, R. Baldev, Synthesis of aqueous and nonaqueous iron oxide nanofluids and study of temperature dependence on thermal conductivity and viscosity, J. Phys. Chem. C 114 (2010) 18825–18833.

[16] D. Singh, E. Timofeeva, W. Yu, J. Routbort, D. France, D. Smith, J.M. Lopez-Cepero, An investigation of silicon carbide-water nanofluid for heat transfer applications, J. Appl. Phys. 105 (2009) (64306-1-6).

[17] X. Li, C. Zou, T. Wang, X. Lei, Rheological behavior of ethylene glycol-based SiC nanofluids, Int. J. Heat Mass Transfer 84 (2015) 925–930.

[18] T.S. Sreeremya, K. Asha, A. Peer Mohamed, U.S. Hareesh, S. Ghosh, Synthesis and characterization of cerium oxide based nanofluids: an efficient coolant in heat transport applications, Chem. Eng. J. 255 (2014) 282–289.

[19] L. Pena-Paras, J. Taha-Tijerina, L. Garza, D.F. Maldonado-Cortas, R. Michalczewski, C. Lapray, Effect of CuO and Al_2O_3 nanoparticle additives on the tribological behavior of fully formulated oils, Wear 332 (2015) 1256–1261.

[20] S.S.J. Aravind, B. Prathab, B. Tessy Theres, R.K. Sabareesh, D. Sumitesh, S. Ramaprabhu, Investigation of structural stability, dispersion, viscosity, and conductive heat transfer properties of functionalized carbon nanotube based nanofluids, J. Phys. Chem. C 115 (2011) 16737–16744.

[21] X. Huaqing, C. Lifei, Review on the preparation and thermal performances of carbon nanotube contained nanofluids, J. Chem. Eng. Data 56 (2011) 1030–1041.

[22] J. Neetu, S. Ramaprabhu, Synthesis and thermal conductivity of copper nanoparticle decorated multiwalled carbon nanotubes based nanofluids, J. Phys. Chem. C 112 (2008) 9315–9319.

[23] M.J. Assael, I.N. Metaxa, J. Arvanitidis, D. Christofilos, C. Lioutas, Thermal conductivity enhancement in aqueous suspensions of carbon multi-walled and double-walled nanotubes in the presence of two different dispersants, Int. J. Thermophys. 26 (2005) 647–664.

[24] L. Chen, H.Q. Xie, Y. Li, W. Yu, Applications of cationic gemini surfactant in preparing multi-walled carbon nanotube contained nanofluids, Colloids Surf. A 330 (2008) 176–179.

[25] L.F. Chen, H.Q. Xie, Properties of carbon nanotube nanofluids stabilized by cationic gemini surfactant, Thermochim. Acta 506 (2010) 62–66.

[26] S.T. Huxtable, D.G. Cahill, S. Shenogin, L.P. Xue, R. Ozisik, P. Barone, M. Usrey, M.S. Strano, G. Siddons, M. Shim, P. Keblinski, Interfacial heat flow in carbon nanotube suspensions, Nat. Mater. 2 (2003) 731–734.

[27] H.Q. Xie, H. Lee, W. Youn, M. Choi, Nanofluids containing multiwalled carbon nanotubes and their enhanced thermal conductivities, J. Appl. Phys. 94 (2003) 4967–4971.

[28] A.A. Balandin, Thermal properties of graphene and nanostructured carbon materials, Nat. Mater. 10 (2011) 569–581.

[29] P.M. Sudeep, J. Taha-Tijerina, P.M. Ajayan, T.N. Narayanan, M.R. Anantharaman, Nanofluids based on fluorinated graphene oxide for efficient thermal management, RSC Adv. 4 (2014) 24887–24892.

[30] B. Tessy Theres, S. Ramaprabhu, Investigation of thermal and electrical conductivity of graphene based nanofluids, J. Appl. Phys. 108 (2010) (124308-1-6).

[31] B. Tessy Theres, S. Ramaprabhu, Synthesis and transport properties of metal oxide decorated graphene dispersed nanofluids, J. Phys. Chem. C 115 (2011) 8527–8533.

[32] B. Tessy Theres, S. Ramaprabhu, Experimental investigation of the thermal transport properties of a carbon nanohybrid dispersed nanofluid, Nanoscale 3 (2011) 2208–2214.

[33] T.-T. Jaime, N.N. Tharangattu, G. Guanhui, R. Matthew, A.T. Dmitri, P. Matteo, M.A. Pulickel, Electrically insulating thermal nano-oils using 2D fillers, ACS Nano 6 (2012) 1214–1220.

[34] K.V. Mahesh, R. Rashada, M. Kiran, A.P. Mohamed, S. Ananthakumar, Shear induced micromechanical synthesis of Ti_3SiC_2 MAXene nanosheets for functional applications, RSC Adv. 5 (2015) 51242–51247.

[35] M.W. Barsoum, The $M_{(n+1)}AX_{(n)}$ phases: a new class of solids; thermodynamically stable nanolaminates prog, Solid State Chem. 28 (2000) 201–281.

[36] M.W. Barsoum, T. El-Raghy, The MAX phases: unique new carbide and nitride materials: ternary ceramics turn out to be surprisingly soft and machinable, yet also heat-tolerant, strong and lightweight Am, Science 89 (2001) 334–343.

[37] K.V. Mahesh, S. Balanand, R. Raimond, A.P. Mohamed, S. Ananthakumar, Polyaryletherketone polymer nanocomposite engineered with nanolaminated Ti_3SiC_2 ceramic fillers, Mater. Design 63 (2014) 360–367.

[38] M.W. Barsoum, T. El-Raghy, C.J. Rawn, W.D. Porter, H. Wang, E.A. Payzant, C.R. Hubbard, Thermal properties of Ti_3SiC_2, J. Phys. Chem. Solids 60 (1999) 429–439.

[39] M.W. Barsoum, T. El-Raghy, Synthesis and characterization of a remarkable ceramic: Ti_3SiC_2, J. Am. Ceram. Soc. 79 (1996) 1953–1956.

[40] Dow Chemical Company. <http://www.dow.com/heattrans/support/selection/ethylene-vs-propylene.htm>, (accessed 03.02.2016).

[41] N. Canter, Heat transfer fluids: selection, maintenance & new applications, Tribol. Lubr. Technol. 65 (2009) 28–35.

[42] W. Jingyang, Z. Yanchun, Recent progress in theoretical prediction, preparation, and characterization of layered ternary transition-metal carbides, Annu. Rev. Mater. Res. 39 (2009) 415–443.

[43] M.W. Barsoum, M. Radovic, Elastic and mechanical properties of the MAX phases, in: Annu. Rev. Mater. Res., D.R. Clarke and P. Fratzl (Eds.), Annual Reviews, USA, 2011, pp. 195–227.

[44] A. Amiri, M. Shanbedi, B.T. Chew, S.N. Kazi, K.H. Solangi, Toward improved engine performance with crumpled nitrogen-doped graphene based water–ethylene glycol coolant, Chem. Eng. J. 289 (2016) 583–595.

[45] H. Chen, S. Witharana, Y. Jina, C. Kim, Y. Ding, Predicting thermal conductivity of liquid suspensions of nanoparticles (nanofluids) based on rheology, Particuology 7 (2009) 151–157.

[46] K.S. Suganthi, N. Anusha, K.S. Rajan, Low viscous ZnO–propylene glycol nanofluid: a potential coolant candidate, J. Nanopart. Res. 15 (2013) 1986.

[47] Y.Q. Tan, Y.H. Song, Q. Zheng, Hydrogen bonding-driven rheological modulation of chemically reduced graphene oxide/poly(vinyl alcohol) suspensions and its application in electrospinning, Nanoscale 4 (2012) 6997–7005.

[48] R. Prasher, D. Song, J. Wang, P. Phelan, Measurements of nanofluid viscosity and its implications for thermal applications, Appl. Phys. Lett. 89 (2006) 1331081–1331083.

[49] S. Xiaoliang, W. Mang, X. Zengshi, Z. Wenzheng, Z. Qiaoxin, Tribological behavior of Ti_3SiC_2/(WC-10Co) composites prepared by spark plasma sintering, Mater. Design 45 (2013) 365–376.